Supplement of

Base-state dependence of parameter sensitivity for the Twomey effect in a perturbed parameter ensemble

Wynn et. al

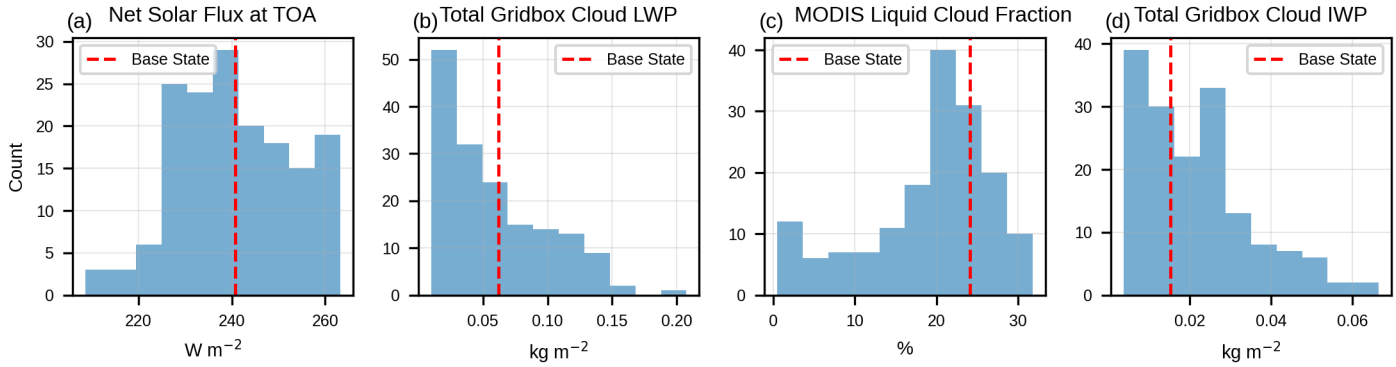

Figure S1. Histograms of global mean ensemble member values for (a) net solar flux at the top of atmosphere (W m^{-2}), (b) total gridbox cloud liquid water path (kg m^{-2}), (c) MODIS liquid cloud fraction (%), and (d) total gridbox cloud ice water path (kg m^{-2}). The red dashed line in each panel indicates the base state value.

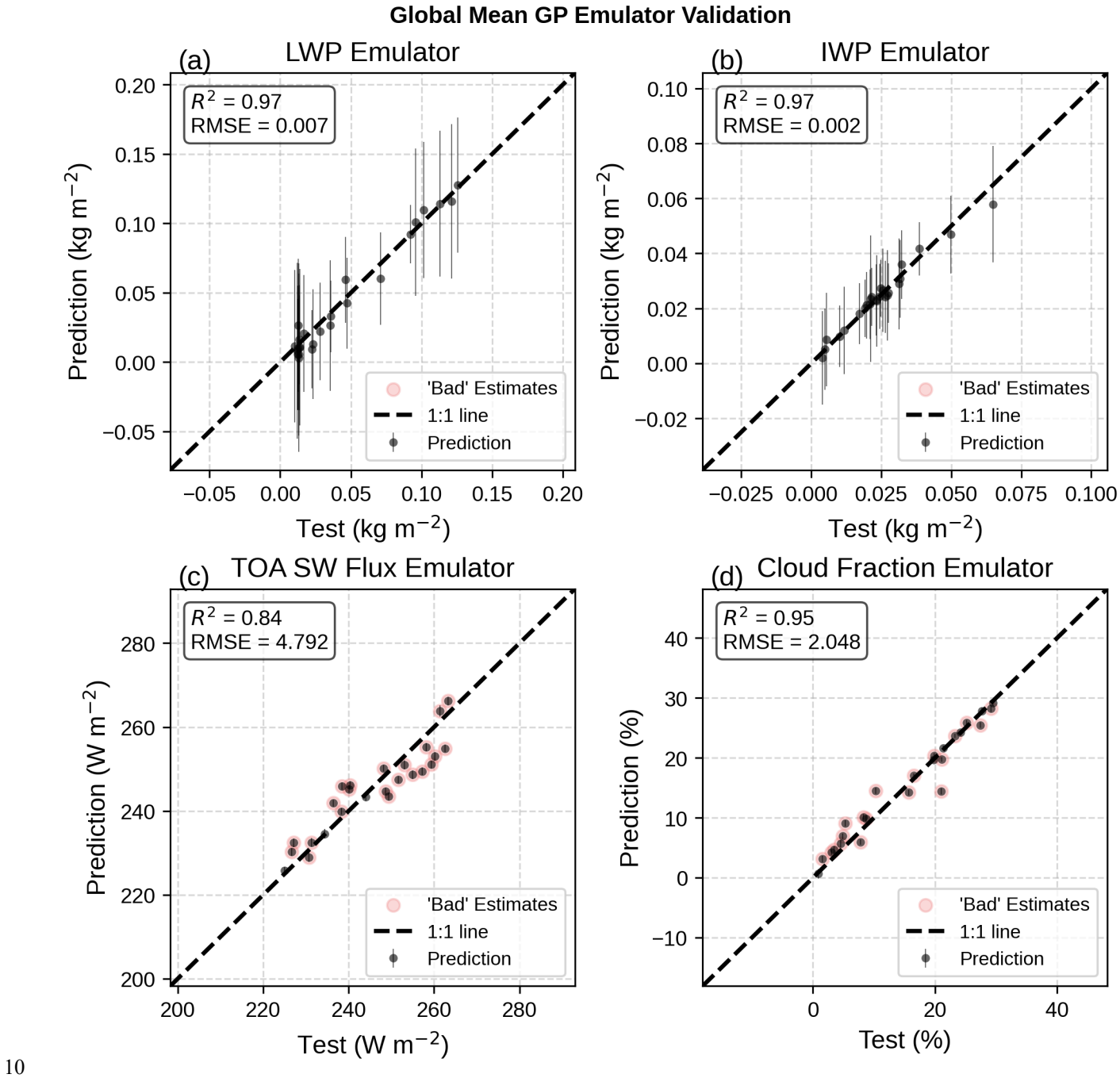

Figure S2. Validation plots for each gaussian process emulators used to create the PD base state. (a) total gridbox cloud liquid water path (kg m^{-2}), (b) total gridbox cloud ice water path (kg m^{-2}), (c) net solar flux at the top of atmosphere (W m^{-2}), and (d) MODIS liquid cloud fraction (%). The vertical grey error bars are the 95% confidence intervals for the emulated uncertainty; red dots represent predictions that fall out of the uncertainty.

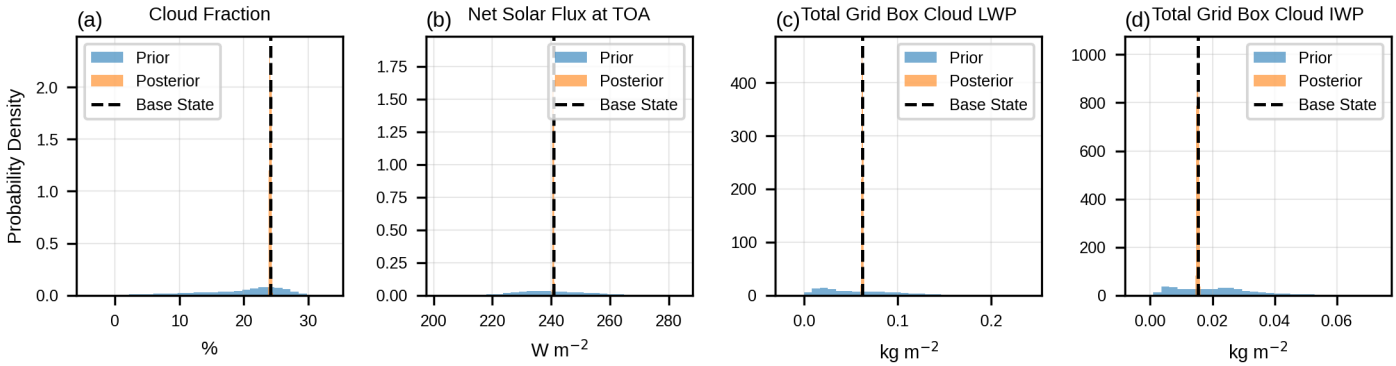

Figure S3. Probability densities of the emulated prior and posterior distributions. Orange shading show the posterior distributions constrained to the base-state model global mean, blue shading show the prior uniform distributions, and the vertical dashed line indicates the base state value to which the posterior was constrained. (a) MODIS liquid cloud fraction (%), (b) net solar flux at the top of atmosphere (W m^{-2}), (c) total gridbox cloud liquid water path (kg m^{-2}), (d) total gridbox cloud ice water path (kg m^{-2}).

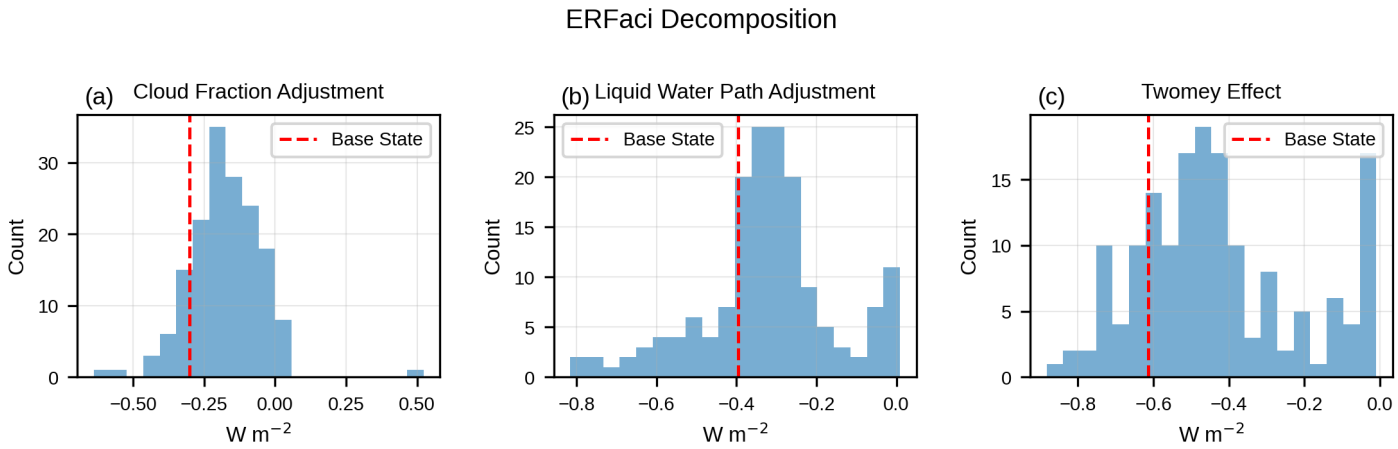

Figure S4. Histograms of global mean ensemble member values for the ERFaci decomposition (a) cloud fraction adjustment (W m^{-2}), (b) liquid water path adjustment (W m^{-2}) (c) Twomey Effect (W m^{-2}). The red dashed line in each panel indicates the base state value.

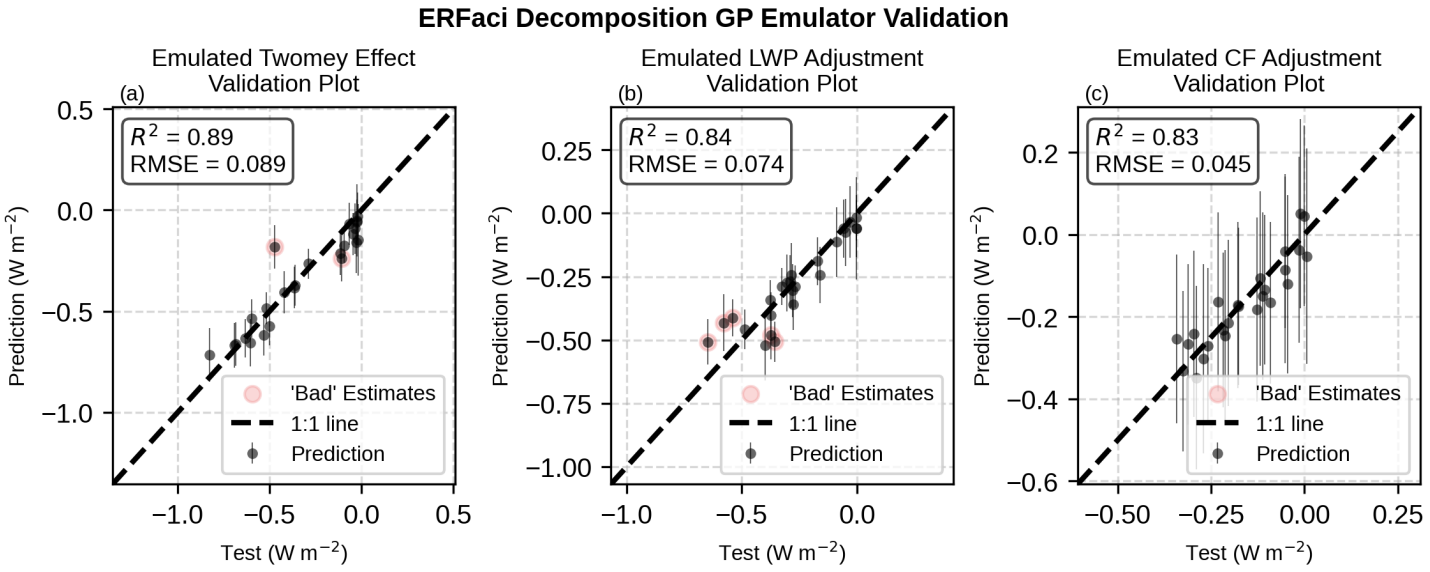

Figure S5. Validation plots for each gaussian process emulators used to create the ERFaci decomposition. (a) Twomey effect (W m⁻²), (b) liquid water path adjustment (W m⁻²), (c) cloud fraction adjustment (W m⁻²), The vertical grey error bars are the 95% confidence intervals for the emulated uncertainty; red dots represent predictions that fall out of the uncertainty.

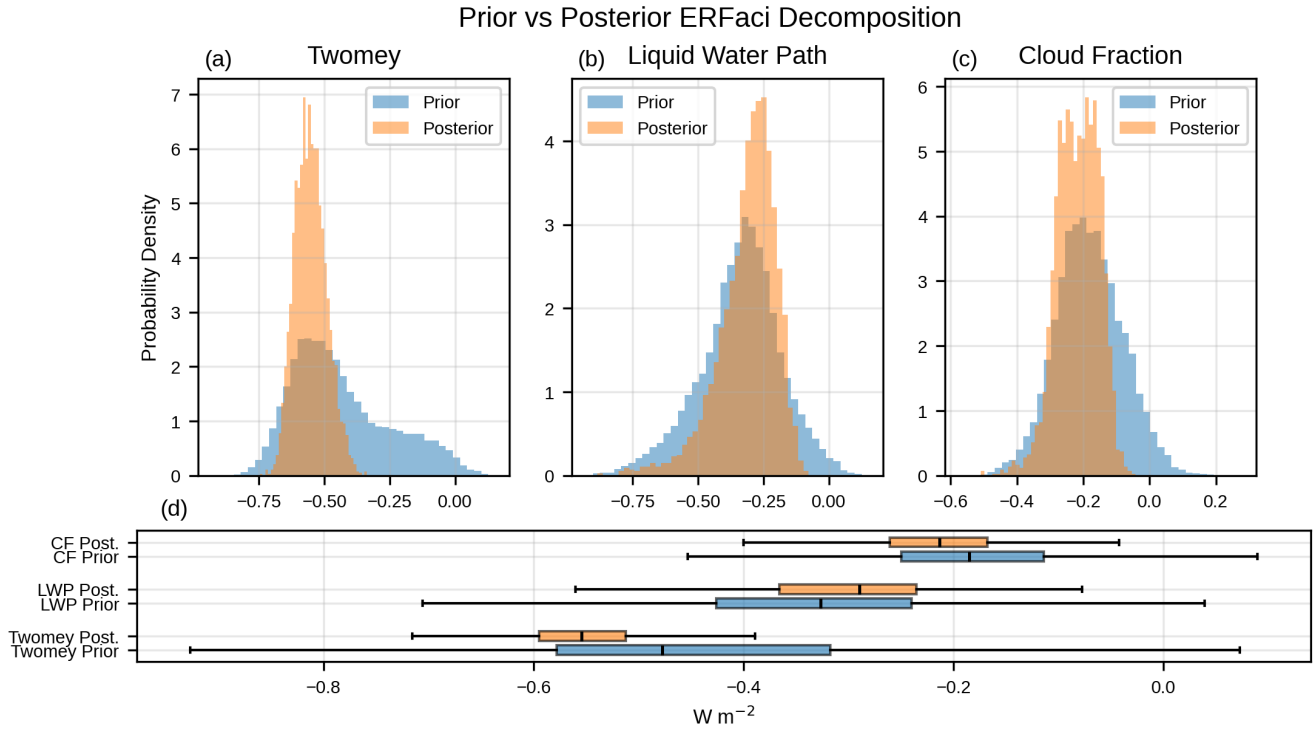

Figure S6. Top panel (a-c) shows the probability densities of the emulated prior and posterior distributions. Orange shading shows the posterior distributions constrained to the base-state observations, blue shading shows the prior uniform distributions. (a) Twomey effect, (b) liquid water path adjustment, (c) cloud fraction adjustment. The bottom panel (d) shows box-and-whisker plots summarizing the prior and posterior distributions for all three components, where boxes indicate the interquartile range, horizontal lines the median, and whiskers the 5th–95th percentile range All in W m⁻².

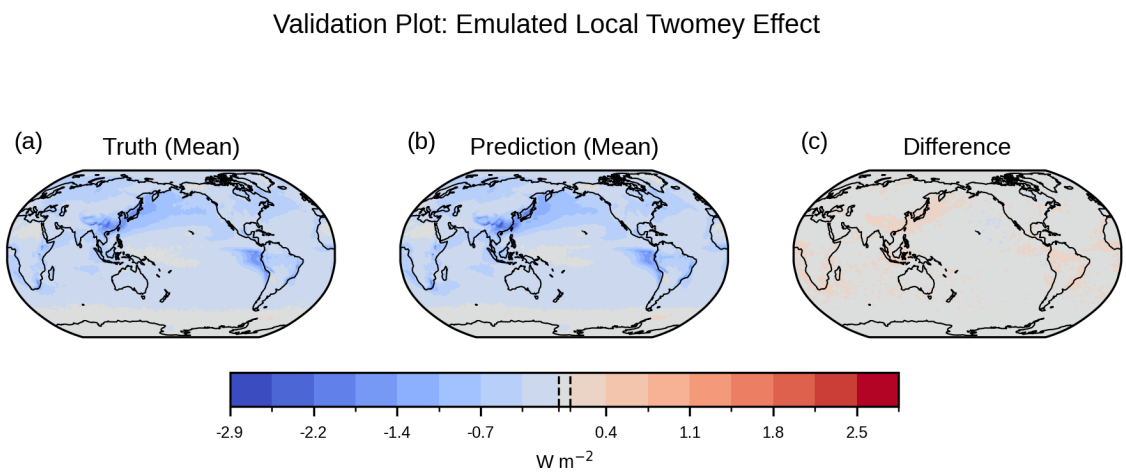

Figure S7. Validation of the local Twomey effect emulator (W m^{-2}). (a) Mean of the held-out test data, (b) mean of the emulator predictions, and (c) the difference between the truth and the predictions.

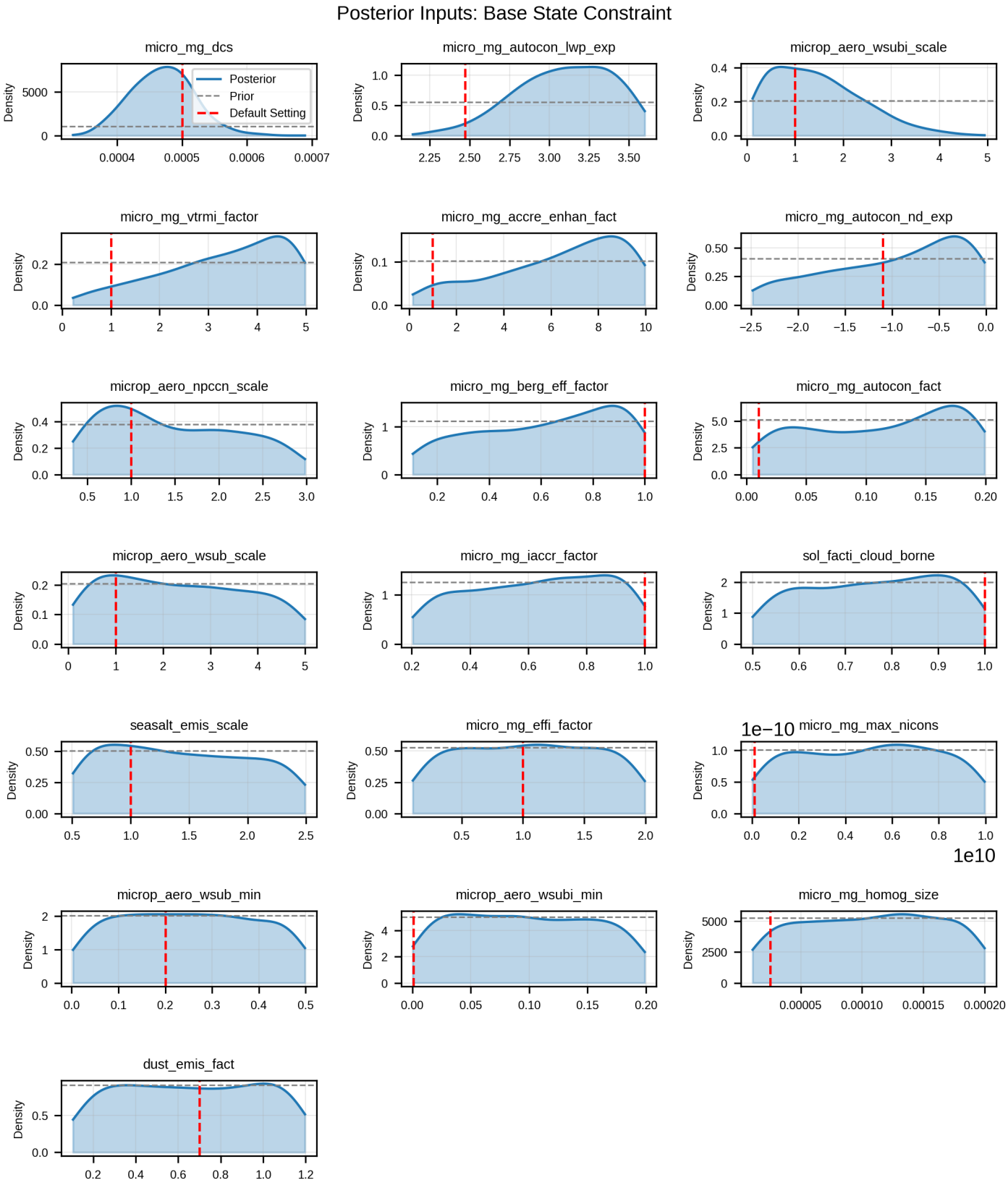
Posterior Inputs: Base State Constraint
micro_mg_dcs
Posterior
Prior
Default Setting
Density
micro_mg_autocon_lwp_exp
microp_aero_wsubi_scale
micro_mg_vtrmi_factor
micro_mg_accre_enhan_fact
micro_mg_autocon_nd_exp
microp_aero_npccn_scale
micro_mg_berg_eff_factor
micro_mg_autocon_fact
microp_aero_wsub_scale
micro_mg_iaccr_factor
sol_facti_cloud_borne
seasalt_emis_scale
micro_mg_effi_factor
1e−10
micro_mg_max_nicons
1e10
microp_aero_wsub_min
microp_aero_wsubi_min
micro_mg_homog_size
dust_emis_fact

Figure S8. Probability densities for each parameter in the posterior base state constrained distribution. Blue curve and shading represents the posterior distribution, dashed grey line represents the uniform prior distribution, and dashed red line represents the default value. Parameters are ordered based on the difference between the prior and posterior distributions, using K-L divergence (Kullback and Leibler, 1951).

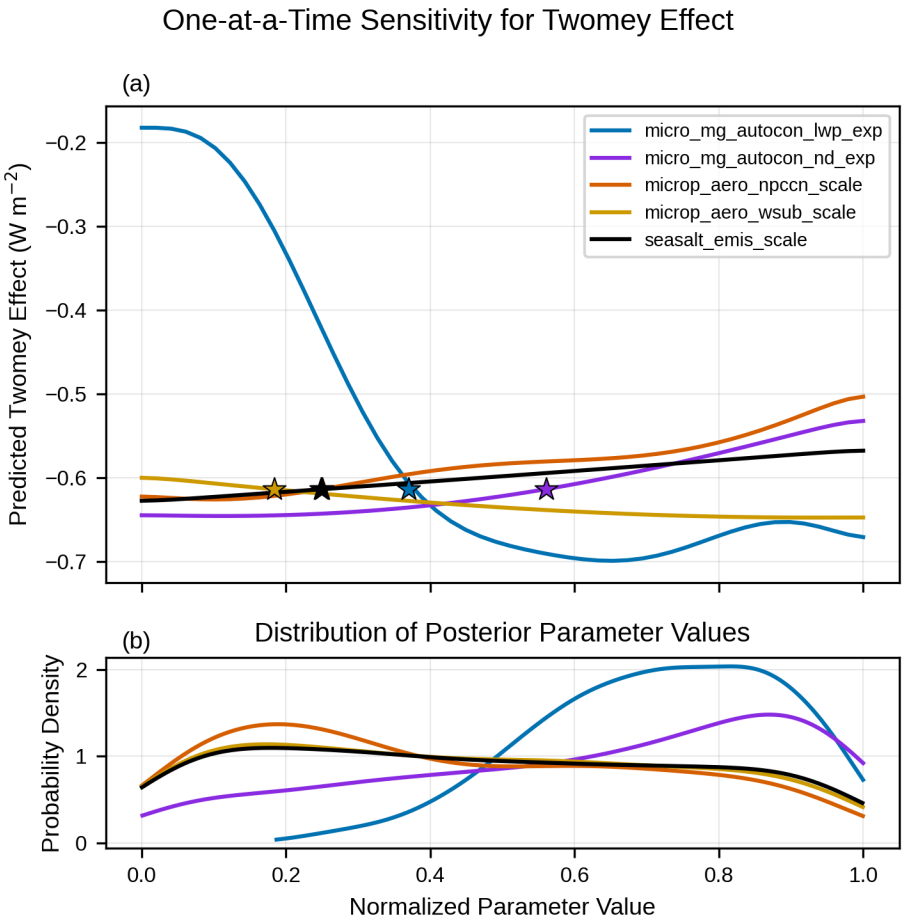

Figure S9. One-at-a-time sensitivity analysis of the Twomey effect. The x-axis the normalized parameter value ranging from 0 to 1 and the y-axis of (a) is the predicted global mean Twomey effect while only varying the labelled parameter. The bottom panel (b) shows probability density functions of the posterior distribution for each of the five parameters along the same x-axis. The stars represent the model's default parameter setting.

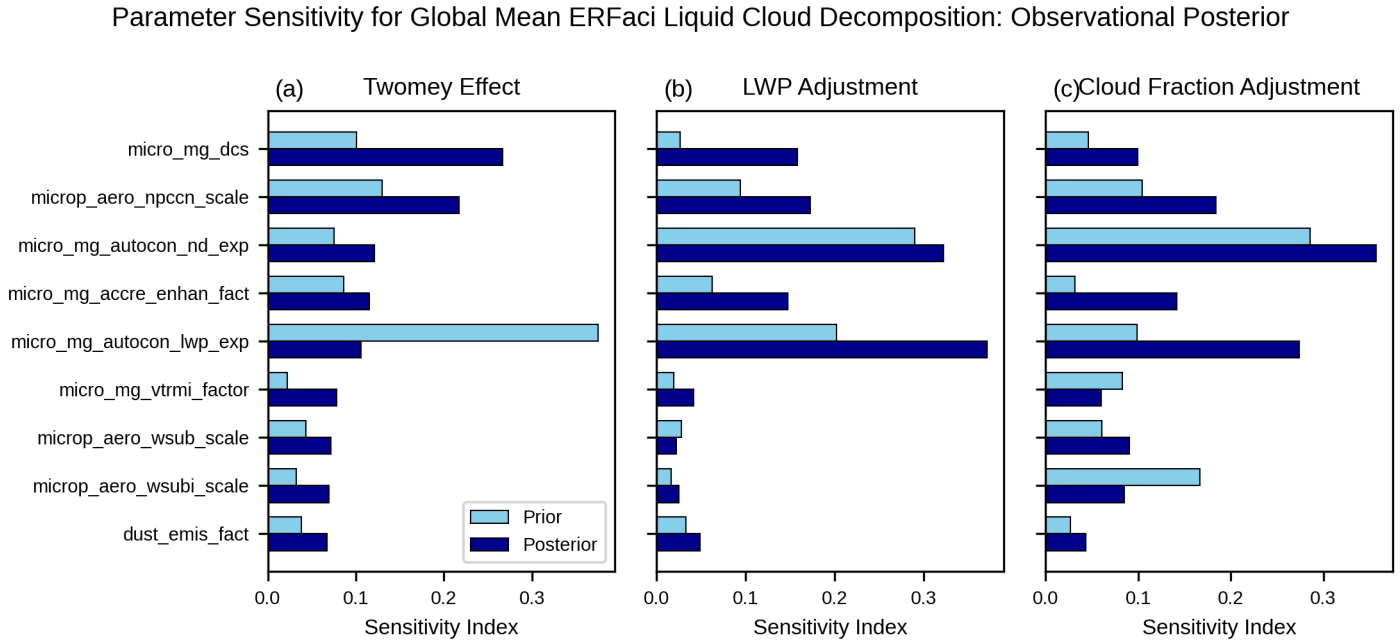

Figure S10. Histograms of parameter sensitivity indices for the liquid cloud decomposed ERFaci forcing, using observational constraints. Light blue represents the sensitivity of each parameter when sampling from the uniform prior distribution. Dark blue represents the sensitivity of each parameter when sampling from the posterior distribution that represents the observational state. Only the 9 most influential parameters are shown.

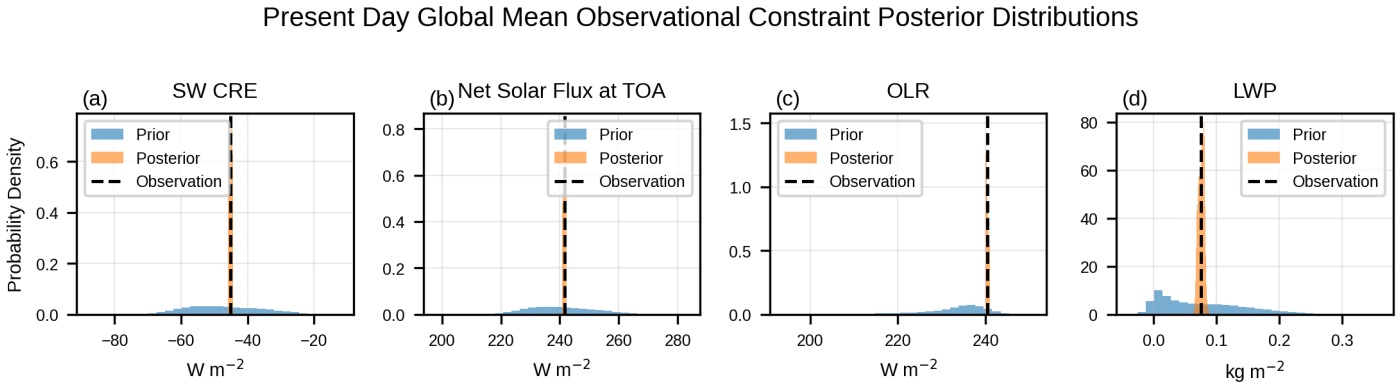

Figure S11. Probability densities of the emulated prior and observational posterior distributions. Orange shading show the posterior distributions constrained to the observation, blue shading show the prior uniform distributions, and the vertical dashed line indicates the base state value to which the posterior was constrained. (a) short wave cloud radiative effect (W m^{-2}),), (b) net solar flux at the top of atmosphere (W m^{-2}), (c) outgoing longwave radiation (W m^{-2}), (d) cloud liquid water path (kg m^{-2}).

Posterior Inputs: Observationally Constrained

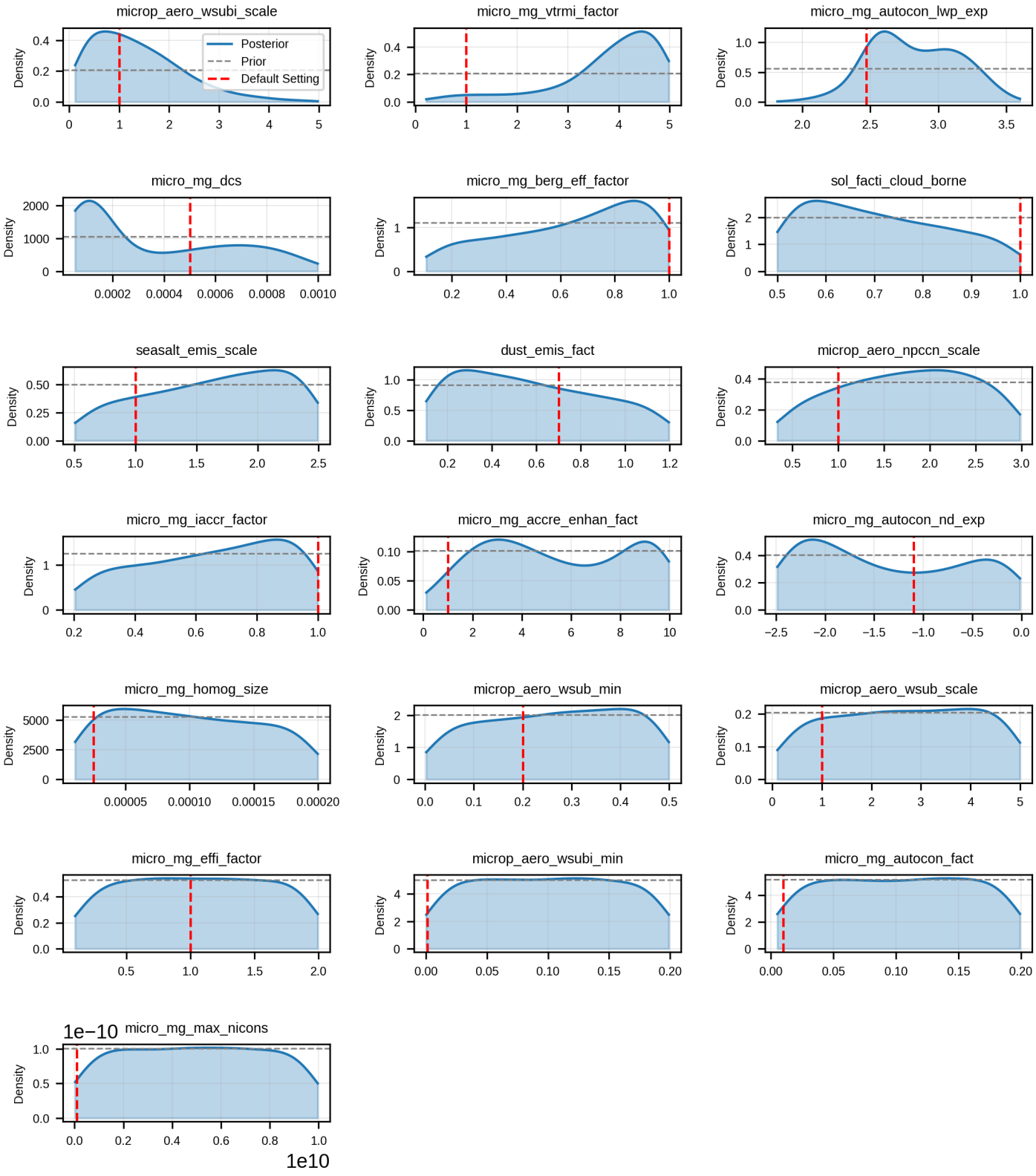

Figure S12. Probability densities for each parameter in the posterior observationally constrained distribution Blue curve and shading represents the posterior distribution, dashed grey line represents the uniform prior distribution, and dashed red line represents the default value for each parameter. Parameters are ordered based on the difference between the prior and posterior distributions, using K-L divergence.

References

S. Kullback. R. A. Leibler. "On Information and Sufficiency." Ann. Math. Statist. 22 (1) 79 - 86, March, 1951. https://doi.org/10.1214/aoms/1177729694